Research Article | Vol. 26, No. 6 | 19 Mar 2018 | OPTICS EXPRESS 7313
Optics EXPRESS

High power single-mode delivery of mid-infrared sources through chalcogenide fiber

A. Sincore,[1,*] J. Cook,[1] F. Tan,[1] A. El Halawany,[1] A. Riggins,[1] S. McDaniel,[2,3] G. Cook,[3] D. V. Martyshkin,[4,5] V. V. Fedorov,[4,5] S. B. Mirov,[4,5] L. Shah,[1,6] A. F. Abouraddy,[1] M. C. Richardson,[1] and K. L. Schepler[1]

[1]*CREOL, The College of Optics & Photonics, University of Central Florida, Orlando, FL 32816, USA*
[2]*Leidos, Dayton, OH 45433, USA*
[3]*Air Force Research Laboratory, Wright Patterson Air Force Base, OH 45433, USA*
[4]*IPG Photonics Mid-IR Lasers, Birmingham, AL 35211, USA*
[5]*Center for Optical Sensors and Spectroscopies, Department of Physics, University of Alabama at Birmingham, AL 35294, USA*
[6]*Currently with Luminar Technologies, Inc., Orlando, FL 32826, USA*
[*]*asincore@knights.ucf.edu*

Abstract: Mechanically robust and low loss single-mode arsenic sulfide fibers are used to deliver high power mid-infrared sources. Anti-reflection coatings were deposited on the fiber facets, enabling 90% transmission through 20 cm length fibers. 10.3 W was transmitted through an anti-reflection coated fiber at 2053 nm, and uncoated fibers sustained 12 MW/cm^2 intensities on the facet without failure. A Cr:ZnSe laser transmitted >1 W at 2520 nm, and a Fe:ZnSe laser transmitted 0.5 W at 4102 nm. These results indicate that by improving the anti-reflection coatings and using a high beam quality mid-infrared source, chalcogenide fibers can reliably deliver ≥10 W in a single mode, potentially out to 6.5 µm.

OCIS codes: (060.2270) Fiber characterization; (060.2390) Fiber optics, infrared; (160.2290) Fiber materials; (060.2280) Fiber design and fabrication; (140.3070) Infrared and far-infrared lasers.

References and links

1. I. Moskalev, S. Mirov, M. Mirov, S. Vasilyev, V. Smolski, A. Zakrevskiy, and V. Gapontsev, "140 W Cr:ZnSe laser system," Opt. Express **24**(18), 21090–21104 (2016).
2. D. V. Martyshkin, V. V. Fedorov, M. Mirov, I. Moskalev, S. Vasilyev, V. Smolski, A. Zakrevskiy, and S. B. Mirov, "High Power (9.2 W) CW 4.15 µm Fe:ZnSe laser," in Conference on Lasers and Electro-Optics, OSA Technical Digest (online) (Optical Society of America, 2017), STh1L.6.
3. V. Fortin, M. Bernier, S. T. Bah, and R. Vallée, "30 W fluoride glass all-fiber laser at 2.94 µm," Opt. Lett. **40**(12), 2882–2885 (2015).
4. F. Maes, V. Fortin, M. Bernier, and R. Vallée, "5.6 W monolithic fiber laser at 3.55 µm," Opt. Lett. **42**(11), 2054–2057 (2017).
5. P. Figueiredo, M. Suttinger, R. Go, E. Tsvid, C. K. N. Patel, and A. Lyakh, "Progress in high-power continuous-wave quantum cascade lasers [Invited]," Appl. Opt. **56**(31), H15–H23 (2017).
6. Y. Bai, N. Bandyopadhyay, S. Tsao, S. Slivken, and M. Razeghi, "Room temperature quantum cascade lasers with 27% wall plug efficiency," Appl. Phys. Lett. **98**(18), 181102 (2011).
7. G. Tao, H. Ebendorff-Heidepriem, A. M. Stolyarov, S. Danto, J. V. Badding, Y. Fink, J. Ballato, and A. F. Abouraddy, "Infrared fibers," Adv. Opt. Photonics **7**(2), 379–458 (2015).
8. S. Shabahang, F. A. Tan, J. D. Perlstein, G. Tao, O. Alvarez, F. Chenard, A. Sincore, L. Shah, M. C. Richardson, K. L. Schepler, and A. F. Abouraddy, "Robust multimaterial chalcogenide fibers produced by a hybrid fiber-fabrication process," Opt. Mater. Express **7**(7), 2336–2345 (2017).
9. S. Sato, K. Igarashi, M. Taniwaki, K. Tanimoto, and Y. Kikuchi, "Multihundred-watt CO laser power delivery through chalcogenide glass fibers," Appl. Phys. Lett. **62**(7), 669–671 (1993).
10. E. Papagiakoumou, D. N. Papadopoulos, and A. A. Serafetinides, "Pulsed infrared radiation transmission through chalcogenide glass fibers," Opt. Commun. **276**(1), 80–86 (2007).
11. L. E. Busse, J. A. Moon, J. S. Sanghera, and I. D. Aggarwal, "Mid-IR high-power transmission through chalcogenide fibers: current results and future challenges," Proc. SPIE **2966**, 553 (1997).
12. F. Chenard, O. Alvarez, and H. Moawad, "MIR chalcogenide fiber and devices," Proc. SPIE **9317**, 93170B (2015).

#314558 https://doi.org/10.1364/OE.26.007313
Journal © 2018 Received 1 Dec 2017; revised 28 Feb 2018; accepted 1 Mar 2018; published 13 Mar 2018

13. A. Sincore, N. Bodnar, J. Bradford, A. Abdulfattah, L. Shah, and M. C. Richardson, "SBS Threshold Dependence on Pulse Duration in a 2053 nm Single-Mode Fiber Amplifier," J. Lightwave Technol. **35**(18), 4000–4003 (2017).
14. P. A. Berry and K. L. Schepler, "High-power, widely-tunable Cr^{2+}:ZnSe master oscillator power amplifier systems," Opt. Express **18**(14), 15062–15072 (2010).
15. R. W. Stites, S. A. McDaniel, J. O. Barnes, D. M. Krein, J. H. Goldsmith, S. Guha, and G. Cook, "Hot isostatic pressing of transition metal ions into chalcogenide laser host crystals," Opt. Mater. Express **6**(10), 3339–3353 (2016).
16. S. B. Mirov, V. V. Fedorov, D. Martyshkin, I. S. Moskalev, M. Mirov, and S. Vasilyev, "Progress in Mid-IR Lasers Based on Cr and Fe-Doped II-VI Chalcogenides," IEEE J. Sel. Top. Quantum Electron. **21**(1), 292–310 (2015).
17. W. H. Kim, V. Q. Nguyen, L. B. Shaw, L. E. Busse, C. Florea, D. J. Gibson, R. R. Gattass, S. S. Bayya, F. H. Kung, G. D. Chin, R. E. Miklos, I. D. Aggarwal, and J. S. Sanghera, "Recent progress in chalcogenide fiber technology at NRL," J. Non-Crystal. Sol. **431**, 8–15 (2016).
18. G. E. Snopatin, M. F. Churbanov, A. A. Pushkin, V. V. Gerasimenko, E. Dianov, and V. G. Plotnichenko, "High purity arsenic-sulfide glasses and fibers with minimum attenuation of 12 dB/km," Optoelectron. Adv. Mater. Rapid Commun. **3**, 669–671 (2009).
19. Engineering Plastic Products – Stock Shapes for Machining (Quadrant Engineering Plastic Products, 1996).
20. D. C. Miller, R. R. Foster, S.-H. Jen, J. A. Bertrand, S. J. Cunningham, A. S. Morris, Y.-C. Lee, S. M. George, and M. L. Dunn, "Thermo-mechanical properties of alumina films created using the atomic layer deposition technique," Sens. Actuators A Phys. **164**(1-2), 58–67 (2010).
21. J. Proost and F. Spaepen, "Evolution of the growth stress, stiffness, and microstructure of alumina thin films during vapor deposition," J. Appl. Phys. **91**(1), 204–216 (2002).
22. F. W. Glaze, D. H. Blackburn, J. S. Osmalov, D. Hubbard, M. H. Black, D. H. B. Francis, and M. H. Black, "Properties of arsenic sulfide glass," J. Res. Nat. Bureau Stds. **59**(2), 83–92 (1957).
23. J. Sanghera, C. Florea, L. Busse, B. Shaw, F. Miklos, and I. Aggarwal, "Reduced Fresnel losses in chalcogenide fibers by using anti-reflective surface structures on fiber end faces," Opt. Express **18**(25), 26760–26768 (2010).

1. Introduction

Mid-infrared (MIR) sources have been demonstrating improved performance and higher output powers. MIR solid-state sources, namely Cr:ZnSe and Fe:ZnSe, have generated output powers of 140 W at 2.5 μm, 32 W at 2.9 μm, and 9 W at 4.1 μm [1, 2]. MIR fiber sources, such as Er:fluoride-glass, have produced output powers of 30 W at 2.94 μm and 5 W at 3.55 μm [3, 4]. Quantum cascade lasers (QCL) can generate >1 W from 3.8 – 10.7 μm [5], with up to 5 W at 4.9 μm [6]. As MIR sources continue to improve in performance, there will be an increasing demand for applications in materials processing, directed energy, remote sensing, laser surgery, and more. For many applications, fiber delivery is beneficial, or even necessary.

Conventional silica fibers do not transmit beyond ~2.4 μm, requiring the use of heavier glass compositions to extend the multiphonon absorption edge into the MIR. Common glasses used for MIR fiber transport are heavy-metal oxides (such as tellurite and germanate glasses), halides (fluorides such as ZBLAN), and chalcogenides (containing sulfur, selenium, tellurium) [7]. While chalcogenide (ChG) fibers allow one of the broadest MIR transmission windows, their mechanical robustness is generally considered unsatisfactory. By employing a multimaterial hybrid fiber fabrication process, low-loss and robust ChG fibers have been drawn. Their 1000x improvement in tensile strength compared to uncoated ChG fibers, as well as preliminary optical loss measurements of <1 dB/m, have been previously reported [8].

Other work has demonstrated power handling through highly multimode ChG fibers with >100 W CW sources [9], long nanosecond sources with a power handling intensity of 38 MW/cm^2 [10], as well as short nanosecond pulses sustaining 500 MW/cm^2 on the facet without damage [11]. However, for this work and many of the envisaged applications, a high degree of beam quality is preferred. Therefore, the robust ChG fibers presented here were designed for coupling and delivery of single-mode beams from common high average power MIR sources. To date, single-mode ChG fibers have transmitted up to 2.1 W at 2 μm, handling intensities of ~5 MW/cm^2 on the facet without damage [12]. The ChG fibers presented here were anti-reflection coated and delivered 10 W at 2053 nm, 1 W at 2520 nm, and 0.5 W at 4102 nm. The intensity on the input facet sustained 12 MW/cm^2 without failure at 2053 nm. Background loss analysis shows that the fiber fabrication process does not

introduce additional losses with respect to the glass preform. Overall, the fabricated ChG fibers are suitable for high power delivery of various MIR sources, potentially out to 6.5 µm.

2. Mechanically robust, single-mode chalcogenide fibers

The ChG fibers were produced by a hybrid fiber fabrication process. First, the double-crucible technique was used to produce high purity glass canes. These were then inserted in a thick polyetherimide (PEI) tube and thermally drawn using a standard fiber draw tower in ambient environment. A description of the fabrication process as well as preliminary mechanical and optical characterization was presented in [8].

The selected core and cladding compositions were $As_{39}S_{61}$ and $As_{38.5}S_{61.5}$ resulting in a numerical aperture of ~0.2. For delivery at λ = 2053 nm and 2520 nm, a fiber with core diameter of 12 µm was drawn, henceforth referred to as ChG-A. Likewise, a ChG-B fiber was drawn with a core diameter of 25 µm for operation at λ = 4102 nm. Figure 1 shows optical images of the ChG fibers with polished facets. The large polymer jacket is what enables the excellent mechanical robustness.

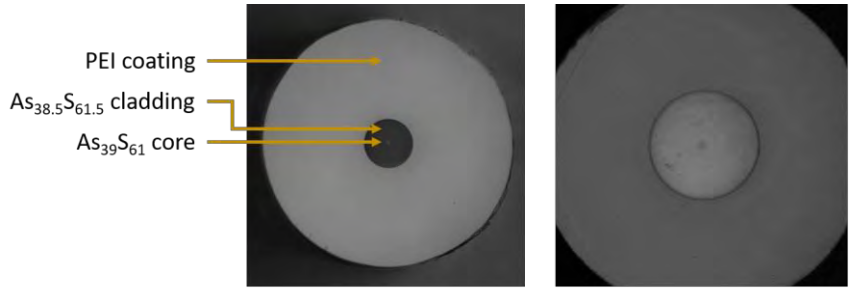

Fiber Diameter (±5%) [µm]	ChG-A		ChG-B
Core	12		25
Cladding	145		310
Coating	700		920
Operating Wavelength [nm]	2053	2520	4102
V-number	3.67	2.99	3.83

Fig. 1. Optical image of the polished chalcogenide fiber facets, along with their dimensions and calculated V-numbers.

The calculated V-numbers indicate the fibers are not strictly single-mode at the tested wavelengths, but may allow the LP_{11} higher-order mode to propagate. The transmitted beam profiles shown in Section 4 demonstrate single-mode guidance for the ChG-A fiber. This suggests that coupling into the fundamental mode was optimal and/or the LP_{11} mode suffers high loss.

For the high power tests, the ChG fibers were separated into 20 cm lengths with flat polished facets. Two ChG-A fibers and one ChG-B fiber were antireflection (AR) coated. The AR-coatings were fabricated by depositing a single-layer of Al_2O_3 on the polished facets with an electron beam evaporator (Temescal FC-2000). As show in Fig. 2, each AR-coated facet should exceed 97% transmission at the design wavelength, based on calculations.

Optics EXPRESS

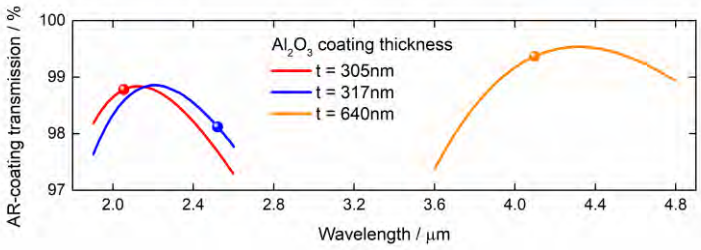

Fig. 2. Theoretical transmission through the deposited AR-coatings using the measured thicknesses (± 5% error). Transmission at the design wavelength is indicated by a circle.

3. Experimental setup for fiber delivery of the MIR sources

Three different high power sources were used in this work. A diode-seeded, Tm:silica fiber amplifier at 2053 nm, a Cr:ZnSe master oscillator power amplifier (MOPA) operating at 2520 nm, and a Fe:ZnSe oscillator at 4102 nm. The architectures for coupling into the ChG fibers are described along with the specifications of each laser system.

3.1 Tm:silica fiber (λ = 2053 nm)

Many MIR materials, such as chalcogenides, transmit down below 2 μm. This is also the longest wavelength attainable in silica. Therefore, this makes Tm:silica fiber lasers an ideal candidate for testing power handling of MIR materials. Furthermore, the results attained by this Tm:fiber system can be carried over to longer wavelength fiber lasers, such as the 30 W Er:fluoride fiber laser emitting at 2.94 μm [3].

The seed source is a 2053 nm diode with sub-MHz linewidth. The seed is amplified through single-mode Tm:silica fiber to over 15 W [13]. The Tm:silica fiber amplifier is single-mode with a delivery fiber having V ≈2.30, giving an output beam $M^2 < 1.1$.

Figure 3 shows the setup for coupling the 2053 nm source into the ChG-A fiber. The mode-field diameter of the Tm:silica fiber amplifier is 11.4 μm. A one-to-one telescope using 11 mm focal length aspheric lenses was used to closely match the 10.6 μm ChG-A mode-field diameter. Fiber coupling simulations using Zemax indicate maximum coupling efficiencies of ~99% are attainable. An optical isolator was required to prevent feedback due to the 17% reflection off the uncoated ChG fiber facet. A light valve consisting of a half-wave plate and polarization beam splitter regulated the power launched into the ChG fiber. Finally, a wedge picked off 1.5% to monitor the launched power and provide calibrated transmission measurements. After accounting for losses through the lenses and free-space optics, 12 W was available to couple into the ChG fiber.

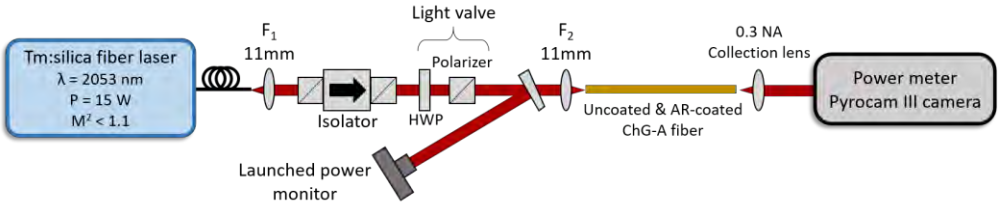

Fig. 3. High power testbed for coupling up to 12 W of a 2053 nm source into the ChG-A fibers. The light valve enabled variable power throughput by rotating the half-wave plate (HWP). An isolator was necessary to prevent instabilities caused by back reflections off the uncoated ChG facet.

3.2 Cr:ZnSe MOPA (λ = 2520 nm)

The 2520 nm source was based on a Cr:ZnSe oscillator and power amplifier, as described in [14]. The oscillator had a free-running emission wavelength at 2520 nm, with spectral

bandwidth under 0.5 nm. The gain medium was produced by the techniques outlined in [15], requiring no frequency stabilization to maintain the output wavelength and narrow linewidth operation. It was operated at a low output power of ~700 mW to maintain optimal beam quality, then subsequently amplified to >4 W by the power amplifier. The amplified output had an M^2 ≈1.4. Imaging the output beam profile revealed beam distribution fluctuations, similar to those observed in [14], but to a lesser extent. These spatial mode fluctuations will be an important issue for coupling high powers into single-mode ChG fiber, as discussed in Section 6.

The source beam waist was located inside the final amplifier gain medium, and was estimated to be ~250 µm diameter based on the M^2 measurements taken after the amplifier. Zemax fiber coupling simulations were used to determine the optimal lens combination for focusing into the ChG fiber with a 4 mm black diamond aspheric lens. Given the available optics coated for 2.5 µm, Zemax simulations indicated the four-lens telescope shown in Fig. 4 could provide coupling efficiencies of ~98%. The optical system could be simplified by replacing the first three lenses with a 75 mm CaF_2 lens. After collimation, a calibrated percentage was picked off to monitor the launched power during transmission measurements. There was no isolator available at this wavelength, so only the AR-coated ChG-A fiber was tested to avoid issues from back reflections.

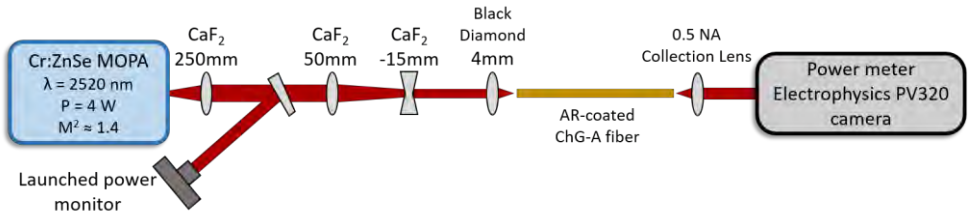

Figure 4. A four lens telescope was used for coupling up to 3.5 W of a 2520 nm Cr:ZnSe MOPA into the ChG-A fiber.

3.3 Fe:ZnSe oscillator (λ = 4102 nm)

The 4102 nm source was a liquid nitrogen cooled Fe:ZnSe oscillator, similar to those reported in [16]. The wavelength was stabilized by a diffraction grating, which could be rotated to tune the output from 3.7 – 4.6 µm. The oscillator produced up to 1.1 W output power at 4102 nm with $M^2 \leq 1.4$.

The beam waist was located at the output coupler with a diameter of ~4.6 mm and was quasi-collimated with 0.9 mrad divergence. This is much larger than the 21.6 µm ChG-B mode-field diameter, therefore requiring a ~200x de-magnification telescope. However, only two optics coated for 4 µm were available; a 150 mm focal length CaF_2 lens and 5.95 mm focal length black diamond aspheric lens, as shown in Fig. 5. Nonetheless, fiber coupling simulations using Zemax indicate with proper lens spacing ~96% coupling efficiencies are attainable, but with an imaging system length over 1 meter. The optical system could be greatly simplified with custom optics, or by first using a high NA lens to generate a small focal point that could be re-imaged into the fiber with off-the-shelf optics.

The Fe:ZnSe oscillator output power was kept at 1.1 W to maintain the same beam quality, and a discrete-step variable attenuator consisting of stacked partially reflecting mirrors was used to vary the launched power. Both uncoated and AR-coated ChG-B fibers were tested. The transmitted beam was measured and viewed directly after the output facet because no collection lens was available.

Optics EXPRESS

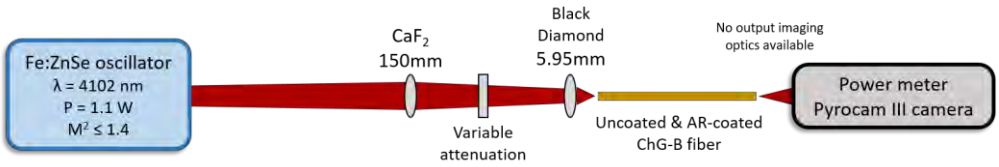

Fig. 5. The Fe:ZnSe oscillator was maintained at 1.1 W and directed through a variable attenuator to vary the power launched into the ChG-B fiber.

4. Results on high power MIR delivery through single-mode ChG fibers

4.1 Tm:silica fiber (λ = 2053 nm)

Two uncoated and one AR-coated ChG-A fibers with 20 cm lengths were investigated. As shown in Fig. 6, the uncoated fibers had an average transmission of 65.5 ± 0.2% and delivered ~8 W. The maximum theoretical transmission, with 100% coupling efficiency and no background loss, is ~70.8% because of Fresnel reflections. The background loss can then be estimated from the transmission measurements. Assuming a high coupling efficiency of 97 ± 3% into the ChG fiber, the estimated background loss at 2053 nm is 1.0 ± 0.7 dB/m. This agrees with the ~0.95 dB/m previously measured using the cut-back method in [8].

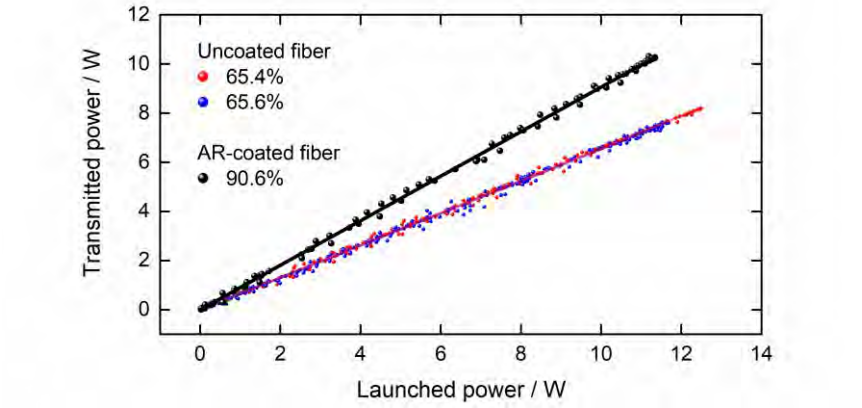

Fig. 6. Measured transmission of the 2053 nm source through 20 cm lengths of ChG-A fiber. AR-coating the fiber enables >90% transmission and 10.3 W delivery. The uncoated fiber sustained intensities of ~12 MW/cm^2 without failure.

The AR-coated fiber demonstrated excellent transmission of 90.6 ± 0.3%, enabling delivery of 10.3 W through the ChG-A fiber. Following from the previous assumptions of 97 ± 3% coupling efficiency and 1.0 ± 0.7 dB/m propagation loss, the AR-coating transmission is estimated to be 99 ± 3%. This agrees with the calculated results from Fig. 2. Inspecting the facet after many high power exposures revealed cracking on the input AR-coated facet, which is further discussed in Section 6.

The output beam profile was single-mode with less than 5% cladding light at low power. Cladding light was measured using a variable aperture on the imaged output and measuring power with the aperture open relative to closed. It was not possible to solely excite the LP_{11} mode, and no noticeable contribution of the LP_{11} mode was observed in combination with the LP_{01} mode. It was found that cladding light increased as the launched power increased, shown in Fig. 7. At maximum transmitted power, ~20% was located in the cladding. This was caused by thermal lensing in the molded aspheric lenses (Thorlabs A397TM-C). This was verified by increasing the optical power on the F_1 collimating lens (see Fig. 3) while the light valve

restricted the power to 100 mW on the remaining optical components. This issue can be prevented by using low-OH^- optics, such as Infrasil or Suprasil lenses.

Overall, the results indicate that the ChG fibers can sustain intensities of 12 MW/cm^2 on the uncoated facet and deliver >10 W. With high quality infrared optics, the ChG fibers are expected to enable >95% coupled into the fundamental mode at high powers.

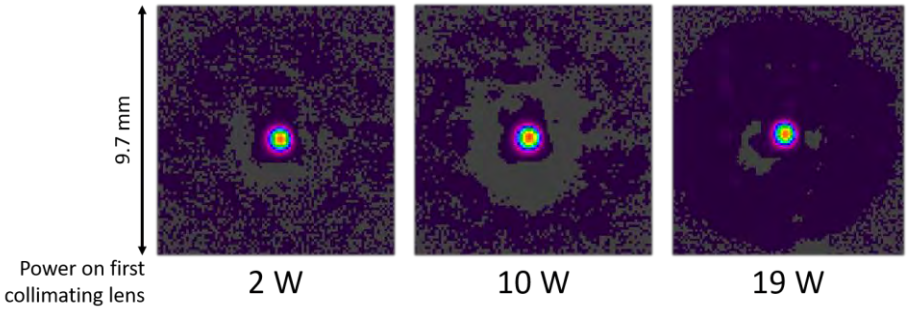

Fig. 7. Transmitted beam profiles of the 2053 nm source through the ChG-A fiber. Thermal lensing in the molded aspheric lenses causes an increase in cladding light at high powers (note that gray is a lower intensity than dark purple). Measurements at low power indicate >95% can be coupled into the fundamental ChG mode.

4.2 Cr:ZnSe MOPA (λ = 2520 nm)

One AR-coated ChG-A fiber with 20 cm length was tested. As shown in Fig. 8, transmission through the fiber was initially 89.4 ± 1.9%. This agrees with the 90.6% measured using the 2053 nm source, indicating the AR-coatings have similar transmission. However, after coupling ~1.3 W the transmission significantly reduced. Inspecting the fiber facet revealed cracking in the AR-coating and damage features in the polymer coating, which is discussed further in Section 6. Even so, the damaged fiber facet sustained multi-Watt transmission without total failure (no transmission through the fiber). This illustrates the integrity of the fiber for power handling, and that the facet is the primary limitation.

Also shown in the Fig. 8 inset is the transmitted beam profile at ~1 W, demonstrating a Gaussian profile. The LP_{11} mode could not be excited similar to the 2053 nm coupling. Saturating the camera image revealed minimal cladding light and strong core confinement. Processing the camera images suggest ~10% cladding light, but large instrument errors and saturated pixels only allow a rough approximation.

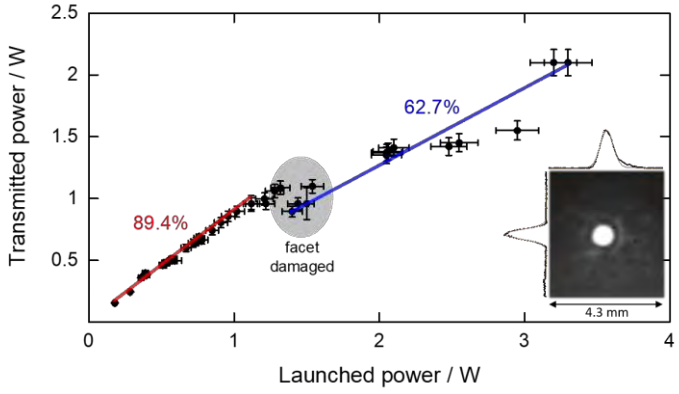

Fig. 8. Measured transmission of the 2520 nm source through 20 cm length of AR-coated ChG-A fiber. Facet damage occurred after coupling ~1.3 W. **Inset:** Beam profile when transmitting 1 W demonstrates strong core confinement with Gaussian profile.

4.3 Fe:ZnSe oscillator (λ = 4102 nm)

Two uncoated ChG-B fibers were tested with lengths of 20 cm and 40 cm. Figure 9 shows the measured power, in which 500 mW was delivered with 45.3 ± 1.3% transmission through the 20 cm length fiber. The 40 cm length fiber had a reduced transmission of 39.0 ± 0.2%, and failed at a coupling power of 1.1 W (the facet ignited). Shown in the Fig. 9 inset is the transmitted beam profile after diverging several millimeters from the output facet. A Gaussian profile is located in the center; however, it is surrounded by a substantial amount of cladding light. The poor coupling likely caused the fiber failure. There was no lens available for imaging the transmitted beam, which would have greatly aided the optical alignment to ensure core coupling. With an improved compact telescope design and better alignment, strong core confinement should be attainable similar to the 2053 nm and 2520 nm source delivery.

From these two different length fibers, the combined core and cladding propagation loss was estimated to be 3.3 ± 0.6 dB/m at 4102 nm. This is significantly greater than both the measured 1.0 ± 0.7 dB/m loss at 2053 nm, and the maximum estimated loss of 1.1 dB/m at 4600 nm reported in [8]. This is due to the sulfur-hydrogen bond (S-H) absorption resonance at 4 µm. In addition, the excessive cladding light increases the measured propagation loss. Section 5 further analyzes this absorption feature, which is commonly found in As_2S_3 glass.

An AR-coated ChG-B fiber was also investigated at low powers of 70 mW, enabling ~62% transmission. This is lower than the 90% measured at 2053 nm and 2520 nm because of the poor coupling and increased propagation loss.

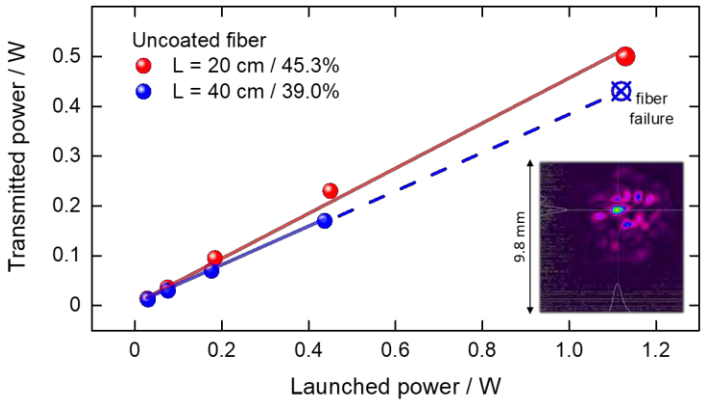

Fig. 9. Measured transmission of the 4102 nm source through a 20 cm and 40 cm length of uncoated ChG-B fiber. Fiber failure occurred when coupling ~1.1 W through the 40 cm length fiber. **Inset:** Beam profile diverging from the ChG output facet. A Gaussian profile is located in the center surrounded by substantial cladding light.

5. Examining the S-H absorption feature at 4 µm

The high propagation loss measured when transmitting the 4102 nm source is due to S-H bonds in the chalcogenide glass. This feature was further examined by taking advantage of the broad wavelength tuning range of the Fe:ZnSe oscillator. Transmission through a 20 cm length ChG-B fiber was measured similar to Section 4.3 at all accessible wavelengths. The relative loss introduced by the S-H bonds can be determined by normalizing the measured output with respect to transmission away from the absorption band (below 3.9 µm and above 4.4 µm). The absolute loss through the fiber cannot be determined with this method.

Figure 10 shows the relative loss of the ChG fiber in the 4 µm region. For comparison, transmission through a 7 mm long sample of the ChG fiber preform measured with Fourier-transform infrared spectroscopy (FTIR) is also shown in Fig. 10. The measured FTIR

transmission includes propagation through both the ChG core and cladding. Therefore, the transmission is normalized identical to the method described above to give relative losses of the absorption features. The S-H absorption is centered at 4023 nm. Another absorption feature is located at 4305 nm, which is attributed to CO_2 impurities in the glass [17]. The lower fluctuations around 4.2 – 4.4 μm occur due to background CO_2 absorption in air, and do not represent loss in the ChG. The high losses of ~12 dB/m do not accurately depict loss for the fiber's fundamental core mode. This is because both measurements include propagation in the glass cladding, which can inflate the measured absorption features by over a factor of 5 [18]. More importantly, comparing the measured loss of the preform and fiber suggests that the fiber drawing process did not add additional loss. This indicates that given a high purity glass cane, mechanically robust ChG fibers can be drawn using this hybrid fabrication method without increasing loss. Figure 10 also shows that the preform can transmit out to 12 μm, with optimal transmission to 6.5 μm.

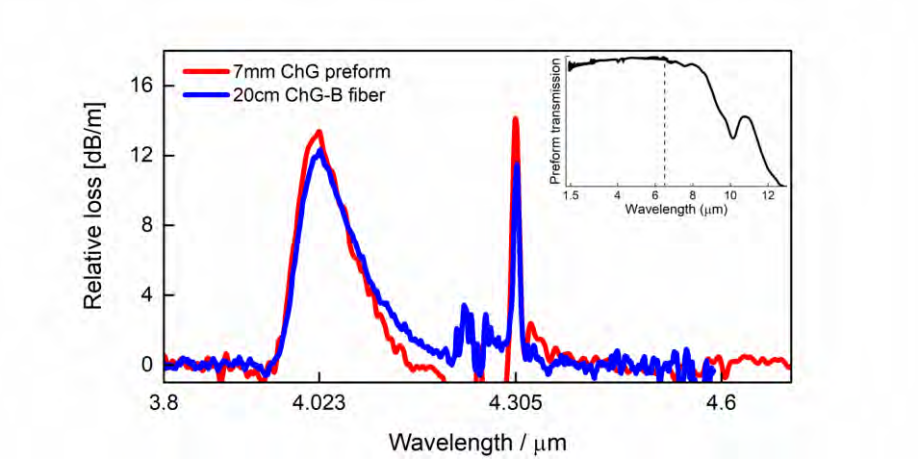

Fig. 10. Measured loss of the ChG-B fiber as compared to the ChG preform. Similar loss measurements between the preform and fiber indicate the hybrid fiber-fabrication process did not introduce additional losses. The high losses of ~12 dB/m is due to both measurements including propagation in the cladding, and do not represent loss of the fundamental core mode. The absorption feature at 4.023 μm is due to S-H bonds, while the feature at 4.305 μm is due to CO_2 impurities. **Inset:** The ChG glass preform has a high transmission window out to 6.5 μm.

6. Design considerations for high power, single-mode MIR fiber delivery

From the results presented in Section 4, an essential factor for delivering high powers into single-mode fibers is the beam quality of the source. Any launched higher-order modes, or unsuitable spatial frequencies, cannot propagate in the ChG fiber core. They scatter into the cladding and inevitably interact with the polymer coating, leading to failure. The beam distribution fluctuations observed in the Cr:ZnSe MOPA output suffered from this coupling issue. On the other hand, the purely single-mode Tm:silica fiber source enabled >95% coupling into the fundamental ChG mode, and handled the maximum power on the facet without failure. Another issue for fiber coupling of solid-state MIR sources, such as Cr:ZnSe and Fe:ZnSe, is that they undergo thermal lensing as the power increases, leading to beam pointing fluctuations and changes in beam waist location. These deviations are imaged through the optical system, which then may launch light outside the fiber core. The Fe:ZnSe oscillator was maintained at maximum power to avoid such potential issues. The lenses used for coupling the Tm:silica fiber source also suffered from thermal lensing, resulting in excess cladding light and stressing the importance for appropriate MIR optics.

Spatial filtering the sources prior to fiber coupling can alleviate the majority of these problems. It would generate a known beam waist location and size while simultaneously filtering excessive spatial frequencies. However, this will also cause a sizeable reduction in available power, and may not be possible depending on the application. Nevertheless, MIR sources are continually being developed to produce diffraction-limited beam quality, which is necessary for high power single-mode fiber delivery. Larger cores could be used to handle more power but at the expense of beam quality, thus resulting in little to no improvement in power density at the target location.

Even with proper facet preparation and MIR source beam quality, high power transmission is hindered by the ~17% reflection at each air-ChG interface. Applying AR-coatings is a common approach to improve overall transmission. In this work, a simple coating approach was undertaken by depositing a single-layer of Al_2O_3. Optimizing the deposition rate produced minimal coating defects across the ChG glass, but cracking remained at the coating-polymer interface. This is attributed to large differences in the coefficient of thermal expansion (CTE). The CTE of PEI polymer is 56 x 10^{-6} K^{-1} [19], which is ~10x greater than the Al_2O_3 coating with a CTE of 4.2 – 6.6 x 10^{-6} K^{-1} [20, 21]. The CTE of As_2S_3 glass is lower at 23 x 10^{-6} K^{-1}, but still ~5x greater than the coating [22]. Even though the AR-coatings had excellent transmission, cracking after high power exposure was a problem. AR-coating failure was the major limitation for further power scaling in these experiments. Figure 11 shows microscope images of the AR-coated ChG-A fibers after exposure to high powers at 2053 nm and 2520 nm. The large discrepancy in power handling between the 2053 nm and 2520 nm test is believed to be due to differences in spatial beam quality. The long, uniform cracks are from cool-down after deposition, and are only prevalent at the coating-polymer interface. The outward propagating cracks near the ChG fiber core were caused by high power laser exposure. As the laser heats the fiber surface, the chalcogenide glass expands more than the coating, causing the coating to crack. Surprisingly, both fibers continued to support multi-Watt transmission without total failure. The AR-coatings could be further improved by choosing a material with a closely matched CTE and optimizing the deposition parameters. Another approach would be to apply AR microstructures [23], which have broadband transmission and circumvent the issue of matching material CTEs.

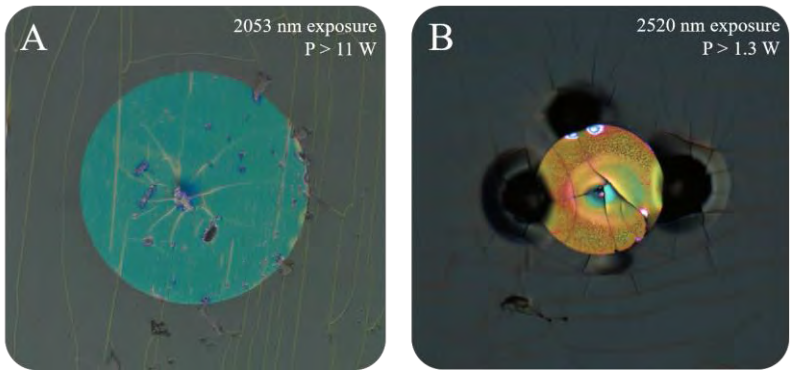

Fig. 11. A) Input facet of the AR-coated ChG-A fiber after exposure to high power at 2053 nm. Cracking in the coating has formed near the fiber core. B) Input facet of another AR-coated ChG-A fiber after exposure to 2520 nm. Cracking is more severe with major damage features in the polymer coating. Both fibers continued to sustain multi-Watt transmission without total failure.

7. Summary

As MIR lasers continue to increase in output power, the capability to fiber deliver these sources with single-mode beam quality will be needed for many applications. Chalcogenide

Optics EXPRESS

fibers can transmit from 1 µm to beyond 6 µm, but suffer from poor mechanical properties and high losses. By using a hybrid fiber fabrication technique, single-mode arsenic sulfide fibers with excellent mechanical properties and low loss were drawn in-house. Three high power sources were coupled into these fibers to examine power handling potential: 2053 nm Tm:silica fiber laser, 2520 nm Cr:ZnSe MOPA, and 4102 nm Fe:ZnSe oscillator. A fiber with 12 µm core diameter was fabricated for operation at 2053 nm and 2520 nm, while a 25 µm core diameter was drawn for 4102 nm. The fibers were also AR-coated by depositing a single-layer of Al_2O_3 on the facets.

A 20 cm length AR-coated fiber delivered >10 W at 2053 nm, with an estimated propagation loss of 1.0 ± 0.7 dB/m. Uncoated fibers handled ~12 MW/cm^2 intensities on the facet without failure. The Cr:ZnSe laser at 2520 nm transmitted over 2 W, with AR-coating damage at ~1.3 W input power. The Fe:ZnSe laser transmitted 0.5 W at 4102 nm, but improper coupling failed to deliver strong confinement in the core. High propagation loss measured at 4102 nm was due to cladding light in combination with the sulfur-hydrogen absorption feature. Measuring this absorption feature in both the drawn fiber and fiber preform show that the fabrication process did not add additional loss. This further supports the hybrid fiber-fabrication process for producing high power handling chalcogenide fibers.

Overall, the results from coupling the Tm:silica fiber laser indicate that given a high quality source, these chalcogenide fibers can reliably deliver 10 W-class systems. High power transmission of common MIR solid-state lasers will further require spatial filtering or ensuring high beam quality (M^2 < 1.1) prior to coupling. The AR coatings were the primary limitation for high power transmission, not the fibers themselves. Improvements will be required for the AR coatings, which experienced cracking after high power exposure due to differences in the coefficient of thermal expansion between the materials.